Off-axis electron holography observation of magnetic microstructure in a magnetite (001) thin film containing antiphase domains

Takeshi Kasama,[1,2,*] Rafal E. Dunin-Borkowski,[2,1] and Wilma Eerenstein[2]
[1]*Frontier Research System, The Institute of Physical and Chemical Research, Hatoyama, Saitama 350-0395, Japan*
[2]*Department of Materials Science and Metallurgy, University of Cambridge, Pembroke Street, Cambridge CB2 3QZ, United Kingdom*
(Received 21 November 2005; revised manuscript received 25 January 2006; published 21 March 2006)

Magnetic remanent states in a self-supporting 25-nm-thick magnetite (001) film containing antiphase domain boundaries (APB's) are investigated using off-axis electron holography in the transmission electron microscope. The observed magnetic microstructure is highly complicated and contains both domain walls and finer-scale magnetic variations. This complexity is attributed in part to a competition between exchange coupling across APB's and the demagnetizing energy of the thin film. Local variations in both the in-plane and out-of-plane components of the magnetic induction in the film are correlated with the positions of the APB's.

DOI: 10.1103/PhysRevB.73.104432 PACS number(s): 75.70.Ak, 75.60.Ch, 42.40.Kw

I. INTRODUCTION

Magnetite (Fe_3O_4) is ferrimagnetic, with a high Curie temperature of 858 K and a high degree of spin polarization.[1,2] Although it has been regarded as an ideal candidate material for use in spin valve devices, attempts to integrate magnetite films into multilayer structures (using MgO substrates) have resulted in disappointing magnetoresistance (MR) values of below 0.5%.[3–5] The small measured MR values do not appear to result from the presence of random spin directions at interfaces in these multilayer structures, which would influence spin polarization and interface scattering, as high-resolution transmission electron microscopy (TEM) has shown that the interfaces are sharp[3] and Mössbauer spectroscopy has shown that the composition and magnetic structure at the interfaces do not differ significantly from that in the interior of the magnetite layers.[6]

However, epitaxial magnetite films grown on MgO substrates are known to contain antiphase domain boundaries (APB's),[6,7] which form at the early stages of growth. At APB's, the oxygen sublattice is undisturbed, but the iron ions are shifted with respect to one another by vectors of the form $\frac{1}{4}\langle 110\rangle$ that lie either in the plane of the film or at 45° to the plane. The presence of these shifts, which are referred to below as in-plane and out-of-plane, respectively, leads to magnetic exchange interactions that are not present in bulk magnetite samples.[8] Some of the exchange interactions are antiferromagnetic,[9] blocking the passage of spin-polarized conduction electrons[10,11] and randomizing magnetic spin directions. The presence of APB's has indeed been shown to have a strong influence on the resistivities of thin films.[12]

Previous studies of the magnetic microstructure of magnetite thin films have been primarily qualitative. Lorentz TEM suggested that 50-nm-thick magnetite films contain distinct magnetic domains that are 2–4 times the antiphase domain (APD) size.[13] In contrast, magnetic force microscopy (MFM) measurements revealed the presence of magnetic domains that were approximately 10 times the APD size in 9.5- and 75-nm-thick films.[14] These results are apparently inconsistent with each other. In neither case was a direct relationship between the APB structure and the magnetic structure established. No direct evidence of the relationship between APB's and magnetic coupling has been obtained to date using any technique.[7,13–16]

In order to address the relationship between magnetic microstructure and the presence of APB's, here we examine a 25-nm-thick magnetite film using off-axis electron holography in the TEM. This technique is capable of measuring the magnetic induction in a thin film quantitatively, with a spatial resolution that can approach 5 nm.[17] We correlate our magnetic measurements with images of the APB structure acquired from the same region of the sample.

II. EXPERIMENTAL DETAILS

Magnetite (001) thin films were grown onto polished MgO substrates using molecular beam epitaxy at a temperature of 250 °C,[18] with uniform thicknesses that were determined during growth from reflection high-energy electron diffraction intensity oscillations. For TEM examination, the films were floated off their substrates[9] and supported directly on Cu TEM specimen grids, without the use of support films. Figure 1(a) shows a bright-field TEM image of such a film. Bandlike contrast in this image corresponds to bend contours, which indicate that the film is slightly bent. Electron diffraction patterns recorded from this film contained extra reflections, as reported elsewhere.[19]

Off-axis electron holograms of several regions of the film were recorded at 300 kV using a Philips CM300ST field-emission gun TEM equipped with an electron biprism and a Lorentz minilens [Fig. 1(b)]. The technique involves illuminating the sample coherently, with the region of interest positioned so that it covers approximately half the field of view. An electron biprism (e.g., a positively charged quartz wire coated with Au) is used to overlap the electron wave that has passed through the sample with a reference wave that has passed only through vacuum. Overlap of the two parts of the electron wave results in the formation of holographic interference fringes, which contain information about both the amplitude and phase shift of the electron wave that has passed through the sample. The phase shift can be used to quantify the in-plane component of the magnetic induction in

 ©2006 The American Physical Society

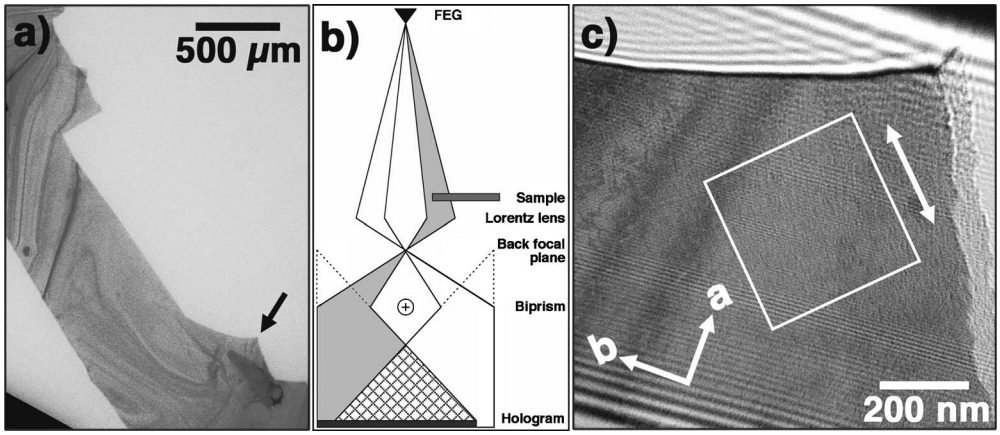

FIG. 1. (a) Low-magnification bright-field image of a self-supporting 25-nm-thick magnetite film. The arrow indicates the area observed using dark-field imaging and off-axis electron holography. (b) Schematic illustration of setup used to generate off-axis electron holograms. The essential components are the field emission gun (FEG) electron source, which is used to provide coherent illumination, and the electron biprism, which is used to overlap the sample and reference waves. The Lorentz lens allows the sample to be examined in magnetic-field-free conditions. (c) Off-axis electron hologram of the area indicated using an arrow in (a). The box indicates the region shown in Figs. 2, 3, 5, 6, and 9. The arrow indicates the direction of the external in-plane field applied using the conventional microscope objective lens, with the specimen tilted by ±30°.

the specimen integrated in the electron beam direction. The Lorentz lens allows holograms of magnetic samples to be acquired at high magnification with the conventional microscope objective lens switched off and the sample in magnetic-field-free conditions. In the present study, electron holograms were acquired using a biprism voltage of 200 V and a holographic interference fringe spacing of 9.1 pixels =4.3 nm [Fig. 1(c)]. Reference holograms were used to remove distortions associated with the imaging and recording system of the microscope. Eighteen holograms were acquired at remanence from each region of interest, after saturating the sample magnetically along either [110] or $[\bar{1}\,\bar{1}\,0]$ [in the direction of the double arrow shown in Fig. 1(c)] using the field of the conventional microscope objective lens, followed by applying a known reverse field. All external fields were applied with the specimen tilted by ±30°. The sample was always tilted back to 0° in zero field and imaged at remanence. The procedure used to record electron holograms and to extract phase information from them is described in detail elsewhere.[17] Conventional two-beam dark-field (DF) images of the film were acquired at 300 kV using a Philips CM30 TEM equipped with a LaB_6 filament. All TEM measurements were performed at room temperature, and the specimen was not subjected to elevated temperatures at any stage of preparation for electron microscopy.

III. RESULTS AND DISCUSSION

DF images of the region of the magnetite film indicated in Fig. 1(c), acquired using {220} and {131} reflections, are shown in Figs. 2(a) and 2(b), respectively. Strongly diffracting regions in the {220} image correspond to the positions of APB's with out-of-plane shifts, 55% of which are visible in this image. In contrast, the {131} image reveals APB's with both in-plane and out-of-plane shifts, 50% of which are visible.[9] When taken together, the two images reveal approximately 80% of all of the APB's that are present in the film. Figure 2 shows that the APD's have a wide range of shapes and an average size of approximately 25 nm. Their boundaries, many of which have straight sections, have measured widths of between 1 and 10 nm, with the larger values corresponding to APB's that are inclined to the film normal by angles of up to ~22°. The presence of such a high density of APB's is thought to be responsible for the absence of a Verwey transition in this sample.[12]

Figure 3 shows magnetic induction maps recorded from the same region of the film using off-axis electron holography. Eight different magnetic remanent states are shown. Images (a)–(d) were acquired after saturating the film upwards and then applying in-plane fields of (a) 32, (b) 192, (c) 299, and (d) 1048 Oe downwards (referred to as +32, +192, +299 and +1048 Oe, respectively). Images (e)–(h) were acquired after saturating the film downwards and then applying external fields of (e) 0, (f) 85, (g) 192, and (h) 1048 Oe upwards (referred to as −0, −85, −192, and −1048 Oe, respectively).

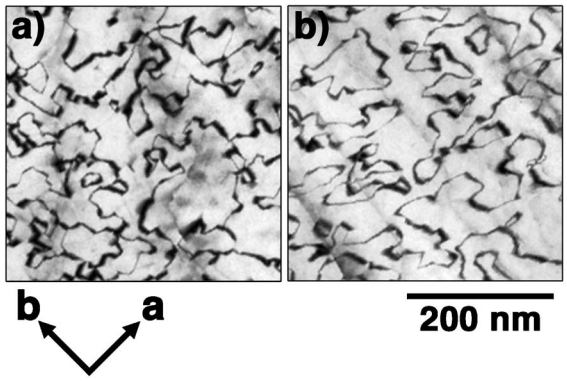

FIG. 2. Dark-field images of the area indicated by the box in Fig. 1(c), acquired using (a) {220} and (b) {131} reflections. The dark contrast corresponds to the positions of APB's.

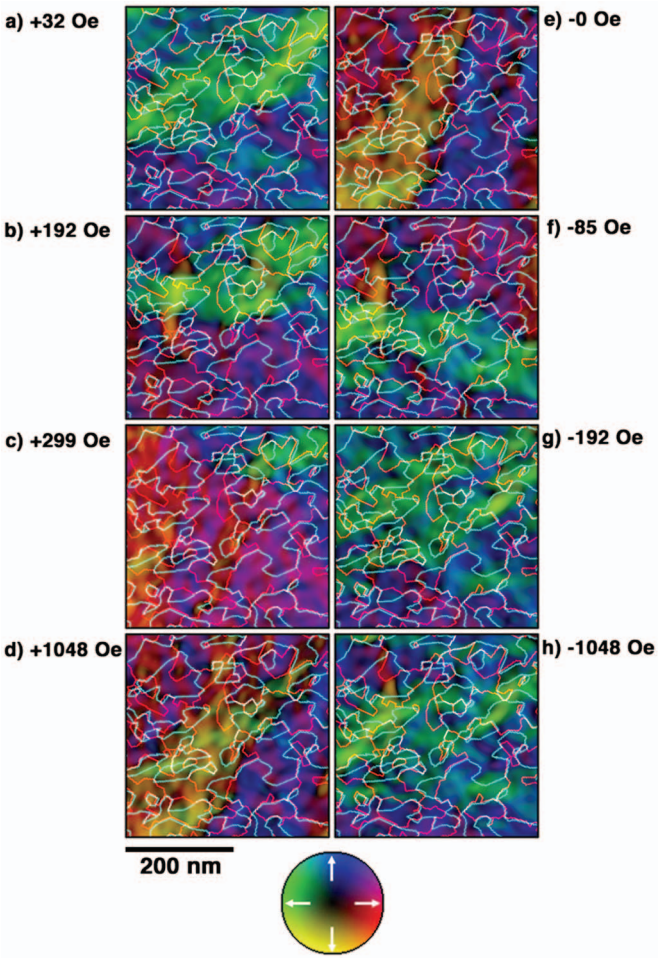

FIG. 3. (Color) Magnetic induction maps of remanent states recorded using off-axis electron holography from the region indicated in Fig. 1(c). The images were acquired after saturating the film magnetically with a large field and then applying in-plane fields of (a) +85, (b) +192, (c) +299, (d) +1048, (e) −0, (f) −85, (g) −192, and (h) −1048 Oe to the specimen (see text for details). The direction of the measured magnetic induction in the film is shown according to a color wheel (red = right, yellow = down, green = left, blue = up). The thin red and white lines in each image correspond to APB's with out-of-plane shifts, while thin blue lines correspond to in-plane shifts.

In each image, the color indicates the direction of the measured induction, according to the color wheel shown at the bottom of Fig. 3. The induction maps, which were generated by differentiating the measured holographic phase shift in two orthogonal directions,[17] reveal subtle features in the magnetic microstructure that may not be discernible using techniques such as the Fresnel mode of Lorentz microscopy or MFM. In contrast to the examination of patterned magnetic nanostructures, the mean inner potential contribution did not have to be subtracted from each recorded phase image because the film thickness was uniform across the field of view. The thin red and blue lines that have been added to each image in Fig. 3 correspond to the positions of the APB's shown in the {220} and {131} DF images in Figs. 2(a) and 2(b), respectively. White—i.e., superimposed (or closely adjacent) red and blue—lines correspond to the positions of

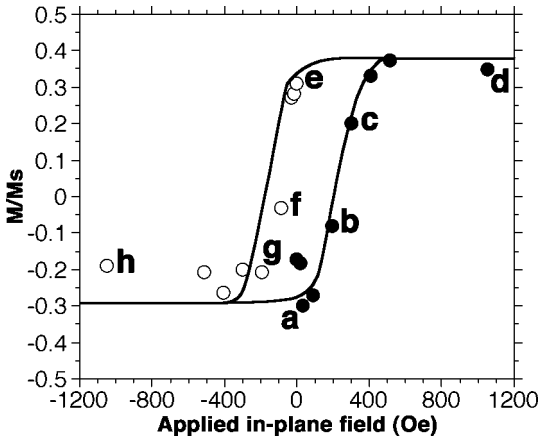

FIG. 4. Remanent hysteresis loop obtained by plotting the average measured magnetic induction in the film, in the direction of the applied field, within an area 500×380 nm in size, as a fraction of that expected for a 25-nm-thick magnetite film. The letters correspond to the eight individual figures shown in Fig. 3. The graph shows the ratio of the measured magnetization (M) to the expected saturation magnetization (M_S), plotted as function of the in-plane component of the field applied to the film before recording the magnetic induction maps with the sample at remanence. The open and solid circles correspond to opposite directions of the applied in-plane field.

APB's that are visible in both the {220} and {131} images. Accordingly, thin red and white lines correspond to out-of-plane shifts, while thin blue lines correspond to in-plane shifts.

The remanent magnetic states shown in Fig. 3 are highly complicated. Irrespective of the magnitude of the applied field, the films are never saturated magnetically at remanence. In addition, the magnetic microstructure does not reverse exactly when similar external fields are applied in opposite directions [e.g., Figs. 3(d) and 3(h)]. Figure 3 shows both coarse-scale magnetic domains (typically at least 100–350 nm in size) and finer-scale magnetic contrast.

Figure 4 shows a remanent hysteresis loop measured directly from the same electron holographic phase images that were used to generate the magnetic induction maps shown in Fig. 3. The horizontal axis is the in-plane component of the field applied to the films before removing the external field and recording the magnetic induction maps at remanence. The vertical axis is the ratio of remanent magnetization to saturation magnetization (M/M_S), calculated from the average gradient of each phase image evaluated perpendicular to the direction of the applied in-plane field. Open and solid circles correspond to opposite directions of the applied in-plane field. The loop tends towards a value of ~0.3, which is slightly lower than that reported previously for a 75-nm-thick magnetite film (0.42).[14] This discrepancy may result in part from the presence of magnetic domains in this region of the specimen, which may in turn be stabilized by the presence of the corner of the thin film close to the region of interest. The measured coercivity of remanence is ~200 Oe, in reasonable agreement with a bulk measurement of 150 Oe for the coercivity of a 13-nm-thick film[7] and 300 Oe for a 75-nm-thick film.[14] Although there is no independent confir-

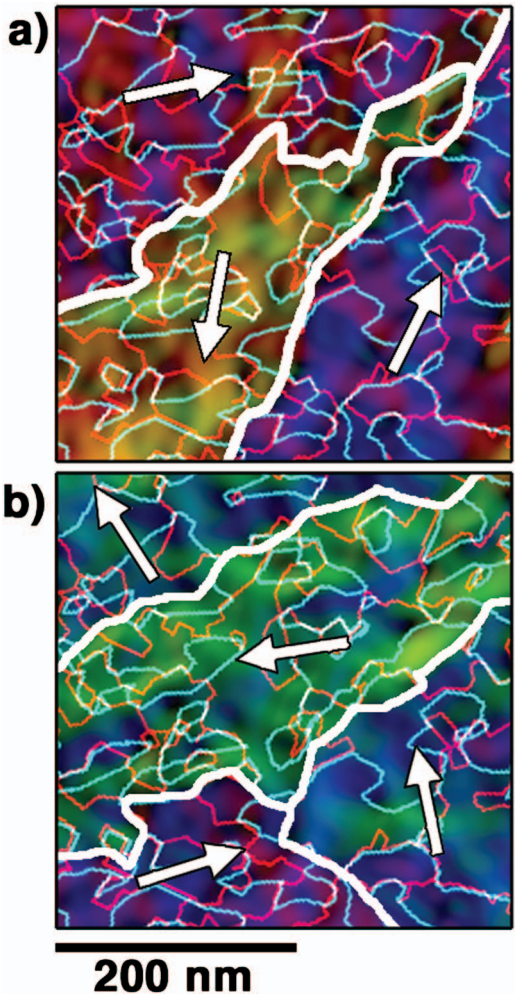

FIG. 5. (Color) Magnetic induction maps recorded using off-axis electron holography after applying in-plane fields of (a) +1048 and (b) −192 Oe, corresponding to Figs. 3(d) and 3(g). The boundaries of coarse magnetic domains are marked. Arrows indicate the average magnetization direction in each coarse domain.

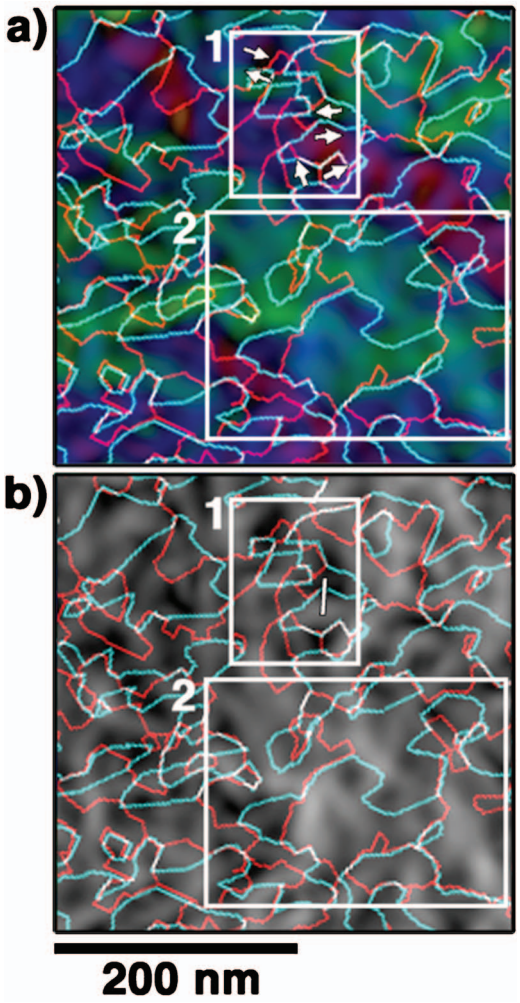

FIG. 6. (Color) (a) Magnetic induction map recorded after applying an in-plane field of −513 Oe. The arrows in box 1 indicate the directions of the measured local magnetic moments. Box 2 shows the presence of larger APD's. (b) Magnitude of the in-plane component of the magnetic induction, derived from (a).

mation that the magnetic properties of the present film are unaffected by removal from its MgO substrate, the lattice mismatch between the film and the substrate is small and removal from the substrate is not expected to result in large changes in the strain of the film. Furthermore, our present magnetic measurements correlate well with previous MFM and nuclear resonance results obtained from films that had not been removed from their substrates.[14,16]

The directions of the coarser domains in Figs. 3(d) and 3(g) are indicated using arrows in Fig. 5. Adjacent domains differ in their average magnetization direction by approximately 90° or 180°. Each domain contains fluctuations in magnetization direction that occur on a scale similar to the size of the APD's in the thin film. The coarse magnetic domains that are visible in Figs. 3 and 5 are between 4 and 14 times larger than the APD's and are similar in size to the magnetic domains observed in similar films using MFM.[14] Although Pan *et al.*[15] also found unusual magnetic contrast that varied on a scale of 100–300 nm, their results were obtained from magnetite films that were 10 times thicker than those examined in the present study and the APD size increases with film thickness.[12] In Fig. 5, the boundaries of the coarse magnetic domains locally follow APB's and often appear on the same APB's in different remanent states (Fig. 3), suggesting that they are pinned at these positions in the film. Domain boundaries that do not appear to coincide with APB's may correspond to the positions of the ~20% of APB's that are not revealed in Figs. 2(a) and 2(b). Alternatively, their presence may result from an inability of the magnetic microstructure to follow crystallographic features such as APB's accurately when their directions change rapidly.

The fine-scale magnetic features visible in Figs. 3 and 5, which have sizes of between 10 and 90 nm, often form as distinct regions within an APD. However, they can also cross between neighboring APD's. Many adjacent fine-scale magnetic features are oriented magnetically approximately 90° to each other, with their boundaries approximately perpendicular to the average magnetization in the bounding coarse domain. This observation suggests that the fine magnetic features are similar in character to magnetic ripple contrast,[20,21]

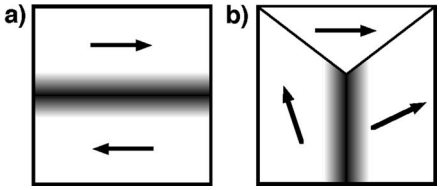

FIG. 7. Schematic diagrams showing APD's coupled antiferromagnetically across APB's. (a) APD's with antiparallel magnetization, corresponding to the middle pair of arrows in Fig. 6(a). (b) APD's with antiparallel local magnetization at a triple APB junction, corresponding to the bottom pair of arrows in Fig. 6(a). The dark regions correspond to significant out-of-plane components of the magnetization in the film.

but that their behavior may be controlled locally by the presence of the APB's.

Figure 6(a) shows a magnetic induction map that corresponds to a −513-Oe field (not shown in Fig. 3). Antiferromagnetic coupling (visible as a 180° change in the local magnetic induction direction) is observed across several APB's, as indicated in box 1, both at APB's with an in-plane shift vector (middle, thin blue line) and at APB's with an out-of-plane shift vector (top, thin red and white lines). The magnitude of the in-plane component of the measured induction is shown in the form of a gray-scale image in Fig. 6(b). Bright intensity corresponds to moments that are fully in-plane, while dark intensity corresponds to moments that are out-of-plane. The vicinities of APB's that exhibit antiferromagnetic coupling are typically associated with a strong out-of-plane component of the magnetization in the film [box 1 in Figs. 6(a) and 6(b)]. In contrast, in larger APD's the local moments far from the APB's tend to lie predominantly in the plane of the film (box 2 in Fig. 6). Reports of significant out-of-plane components of magnetization in Mössbauer measurements[22] may therefore be associated with the presence of antiferromagnetic coupling at APB's. A schematic illustration of such an antiferromagnetic APB configuration is shown in Fig. 7(a). Although in-plane moments in the film are not antiparallel across all APB's [e.g., bottom arrows in box 1 in Fig. 6(a)], this behavior may be influenced by the local crystallography of the specimen (the angles of the APB's with respect to each other) and may still be associated with out-of-plane moments [Fig. 7(b)]. No correlation was observed between the presence of magnetic coupling across APB's and their inclination (their width in the DF images shown in Fig. 2).

Figure 8 shows the variation of the inclination of the magnetization from the plane of the film, inferred from the measured in-plane component of induction and plotted as a function of distance from a single APB along the white line marked in box 1 in Fig. 6(b). The narrow width of the diffraction contrast visible at the position of this APB in Fig. 2 indicates that it runs almost perpendicular through the film. The local moments at the APB are inclined at an angle of almost 90° to the plane of the specimen, gradually rotating back to the specimen plane over a distance of ~17 nm. For this APB, the local moments begin to rotate out of the plane again due to the presence of a neighboring APB. Figure 8 is consistent with a report by Kalev and Niesen[16] of a moment

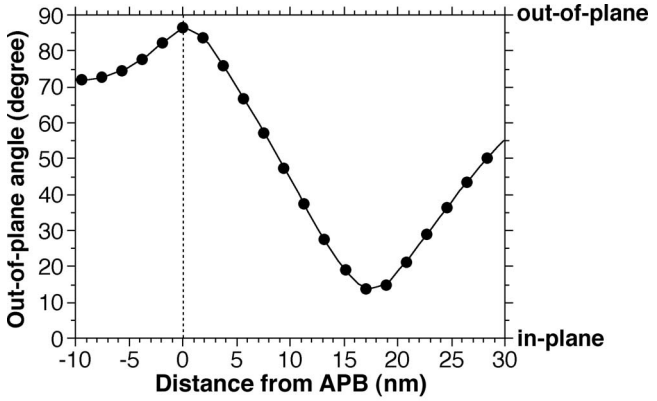

FIG. 8. Angle of the magnetic moment from the film plane plotted as a function of distance from an APB, measured along the line shown in box 1 in Fig. 6(b). This APB is almost perpendicular to the plane of the film.

angle at an APB of 88.5° in zero magnetic field and a distance between out-of-plane angles of 15° and 88.5° of approximately 20 nm. If the distance over which the moments rotate is independent of APD size, then for a given film thickness a larger APD size would correspond to a higher fraction of moments in the plane of the film.

The regions of Fig. 3(g) that correspond to moment angles of >70° from the plane of the film are marked using circles in Fig. 9. White circles correspond to such regions that lie at the positions of APB's, while red circles correspond to other positions in the film, at which APB's may also be present. The remanent state shown in Fig. 9 (corresponding to an in-plane field of −192 Oe) was expected to exhibit a relatively large number of antiferromagnetically coupled do-

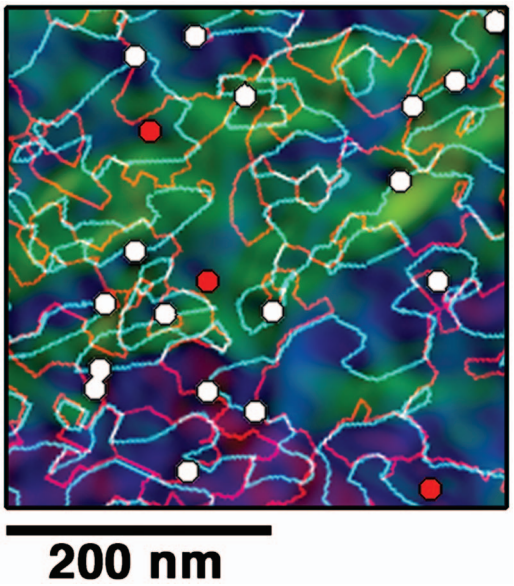

FIG. 9. (Color) Distribution of APB's that have magnetic moment angles of >70° from the film plane, after applying an in-plane field of −192 Oe to the specimen. The white solid circles correspond to antiferromagnetic coupling at APB's, while the red solid circles correspond to antiferromagnetic coupling away from the positions of known APB's.

mains across APB's as the applied field is close to the coercivity of the specimen. However, fewer than 10% of the APB's exhibit antiferromagnetic coupling. Neighboring APD's are expected to couple to each other either antiferromagnetically or ferromagnetically, and the possibility of the occurrence of antiferromagnetic coupling is predicted to be up to 50% theoretically for two domains separated by a single APB.[9] In reality, intersections of three or more APB's are present experimentally (e.g., box 1 in Fig. 6). As shown schematically in Fig. 7(b), if the local moments across one APB are coupled antiferromagnetically, then those at the other two APB's may not be. In such a geometry, magnetic interactions may be much more complicated than across a single APB. The fact that antiferromagnetic coupling is present at fewer APB's than predicted theoretically in Fig. 9 is in agreement with previous experimental results.[13,14,16] Both the presence of a network of APB's and the requirement for minimizing the demagnetizing field associated with out-of-plane moments in a thin film undoubtedly contribute to the complexity of the observed coarse and fine-scale magnetic contrast.

The 180° iron-oxygen-iron superexchange interaction, which is related to antiferromagnetic coupling, is predicted to be very strong,[6,7] suggesting that large magnetic fields should be required to align the moments across an APB ferromagnetically. By comparing Figs. 5(a) and 5(b) and Fig. 9, antiferromagnetic coupling is observed at different APB's in successive remanent magnetic induction maps in the same region of this film, showing that even moderate applied fields are able to change the antiferromagnetic coupling. However, it should be noted that the film was saturated magnetically before recording each magnetic induction map. The continuous increase in magnetization reported in such films with increasing magnetic field is likely to be caused not only by a decrease in domain-wall width[13,16,23] but also by the disappearance of antiferromagnetic coupling across APB's.

With respect to the influence of the magnetic microstructure on the spin polarization of magnetite films and, consequently, on the performance of magnetite films in magnetic tunnel junctions, even though antiferromagnetic coupling is only present at $<10\%$ of the APB's, the area covered by neighboring antiferromagnetically coupled domains is not negligible. As the conduction electrons in such neighboring domains are oppositely polarized, antiferromagnetically coupled APB's will reduce the total spin polarization. Indeed, magnetite films grown on MgO (001) were found[24,25] to have a lower spin polarization than magnetite (111) films that did not contain APB's.[2] Interestingly, even small changes in the positions of the iron ions are predicted to have a strong influence on the band structure and on the spin polarization of such films.[24] Besides antiferromagnetic coupling, local shifts in the positions of iron ions may therefore also affect spin polarization. For this reason, magnetite films containing APB's may not be capable of giving rise to high MR in tunnel junctions. The interface between magnetite and an MgO spacer layer in the tunnel junctions is probably not responsible for the low MR values, as other tunnel junctions that utilize MgO as a spacer layer perform very well.[26,27]

IV. CONCLUSIONS

We have examined antiphase boundaries and remanent magnetic states in a 25-nm-thick magnetite (001) film using dark-field TEM and off-axis electron holography. We observe highly complicated magnetic microstructure in this film. This complexity may result from a competition between magnetic couplings across APB's and the geometry of the thin-film specimen. Coarse magnetic domains are between 4 and 14 times the APD size, while finer-scale magnetic features are between 0.5 and 4 times the APD size. Both antiferromagnetic and ferromagnetic couplings across APB's are present in this specimen, with antiferromagnetic coupling occurring independently of the type of APB, but at less than 10% of the observed APB's. Out-of-plane moments are observed at the positions of a large proportion of the APB's. These moments rotate to in-plane orientations over a distance of approximately 20 nm. The complicated magnetic microstructure is likely to reduce the spin polarization of such magnetite films.

ACKNOWLEDGMENTS

We thank S. Celotto and T. Hibma for discussions and the Royal Society, UK, for financial support.

*Corresponding author. Permanent address: Department of Materials Science and Metallurgy, University of Cambridge, Pembroke Street, Cambridge CB2 3QZ, UK. FAX: +441223334563. Electronic address: tk305@cam.ac.uk

[1] A. Yanase and N. Hamada, J. Phys. Soc. Jpn. **68**, 1607 (1999).
[2] Y. S. Dedkov, U. Rüdiger, and G. Güntherodt, Phys. Rev. B **65**, 064417 (2002).
[3] X. W. Li, A. Gupta, G. Xiao, W. Qian, and V. P. Dravid, Appl. Phys. Lett. **73**, 3282 (1998).
[4] P. J. van der Zaag, P. J. H. Bloemen, J. M. Gaines, R. M. Wolf, P. A. A. van der Heijden, R. J. M. van de Veerdonk, and W. J. M. de Jonge, J. Magn. Magn. Mater. **211**, 301 (2000).
[5] S. Van Dijken, X. Fain, S. M. Watts, K. Nakajima, and J. M. D. Coey, J. Magn. Magn. Mater. **280**, 322 (2004).
[6] F. C. Voogt, T. T. M. Palstra, L. Niesen, O. C. Rogojanu, M. A. James, and T. Hibma, Phys. Rev. B **57**, R8107 (1998).
[7] D. T. Margulies, F. T. Parker, F. E. Spada, R. S. Goldman, J. Li, R. Sinclair, and A. E. Berkowitz, Phys. Rev. B **53**, 9175 (1996).
[8] T. Hibma, F. C. Voogt, L. Niesen, P. A. A. van der Heijden, W. J. de Jonge, J. J. T. M. Donkers, and P. J. van der Zaag, J. Appl. Phys. **85**, 5291 (1999).
[9] S. Celotto, W. Eerenstein, and T. Hibma, Eur. Phys. J. B **36**, 271 (2003).
[10] M. Ziese and H. J. Blythe, J. Phys.: Condens. Matter **12**, 13 (2000).
[11] W. Eerenstein, T. T. M. Palstra, S. S. Saxena, and T. Hibma, Phys.

Rev. Lett. **88**, 247204 (2002).
[12] W. Eerenstein, T. T. M. Palstra, T. Hibma, and S. Celotto, Phys. Rev. B **66**, 201101(R) (2002).
[13] D. T. Margulies, F. T. Parker, M. L. Rudee, F. E. Spada, J. N. Chapman, P. R. Aitchison, and A. E. Berkowitz, Phys. Rev. Lett. **79**, 5162 (1997).
[14] J. F. Bobo, D. Basso, E. Snoeck, C. Gatel, D. Hrabovsky, J. L. Gauffier, L. Ressier, R. Mamy, S. Visnovsky, J. Hamrle, J. Teillet, and A. R. Fert, Eur. Phys. J. B **24**, 43 (2001).
[15] Q. Pan, T. G. Pokhil, and B. M. Moskowitz, J. Appl. Phys. **91**, 5945 (2002).
[16] L. A. Kalev and L. Niesen, Phys. Rev. B **67**, 224403 (2003).
[17] R. E. Dunin-Borkowski, M. R. McCartney, and D. J. Smith, *Encyclopedia of Nanoscience and Nanotechnology*, edited by H. S. Nalwa (American Scientific, Stevenson Ranch, CA, 2004), Vol. 3, pp. 41–100.
[18] W. Eerenstein, T. T. M. Palstra, T. Hibma, and S. Celotto, Phys. Rev. B **68**, 014428 (2003).
[19] M. L. Rudee, D. J. Smith, and D. T. Margulies, Microsc. Microanal. **6**, 400 (2000).
[20] C. L. Platt, M. R. McCartney, F. T. Parker, A. E. Berkowitz, Phys. Rev. B **61**, 9633 (2000).
[21] N. G. Chechenin, J. T. M. de Hosson, and D. O. Boerma, Philos. Mag. **83**, 2899 (2003).
[22] T. Fujii, M. Takano, R. Katano, Y. Isozumi, and Y. Bando, J. Magn. Magn. Mater. **130**, 267 (1994).
[23] H. Zijlstra, IEEE Trans. Magn. **15**, 1246 (1979).
[24] D. J. Huang, C. F. Chang, J. Chen, L. H. Tjeng, A. D. Rata, W. P. Wu, S. C. Chung, H. J. Lin, T. Hibma, and C. T. Chen, J. Magn. Magn. Mater. **239**, 261 (2002).
[25] M. Fonin, R. Pentcheva, Y. S. Dedkov, M. Sperlich, D. V. Vyalikh, M. Scheffler, U. Rüdiger, and G. Güntherodt, Phys. Rev. B **72**, 104436 (2005).
[26] S. S. P. Parkin, C. Kaiser, A. Panchula, P. M. Rice, B. Hughes, M. Samant, and S.-H. Yang, Nat. Mater. **3**, 862 (2004).
[27] S. Yuasa, T. Nagahama, A. Fukushima, Y. Suzuki, and K. Ando, Nat. Mater. **3**, 868 (2004).